Available online at www.sciencedirect.com
ScienceDirect
Journal of Power Sources 166 (2007) 567–577
JOURNAL OF POWER SOURCES
www.elsevier.com/locate/jpowsour

Preparation and characterisation of chemical manganese dioxide: Effect of the operating conditions

F. Pagnanelli [a,*], C. Sambenedetto [a], G. Furlani [a], F. Vegliò [b], L. Toro [a]

[a] *Department of Chemistry, "La Sapienza" University of Rome, P.le A. Moro, 5, 00185 Roma, Italy*
[b] *Dipartimento di Chimica, Ingegneria Chimica e Materiali, Università degli Studi di L'Aquila, 67040 Monteluco di Roio, L'Aquila, Italy*

Received 22 February 2006; received in revised form 12 January 2007; accepted 17 January 2007
Available online 2 February 2007

Abstract

In this study MnO_2 preparation by chemical methods is investigated for possible applications in dry cell batteries of chemical manganese dioxide (CMD) instead of electrolytic manganese dioxide (EMD). Three preparation procedures were tested: precipitation–oxidation by air plus acid activation (two-step-air), precipitation–oxidation by H_2O_2 plus acid activation (two-step-H_2O_2), precipitation–oxidation by $KClO_3$ (single-step-ClO_3). Replicated factorial designs and related statistical analysis of experimental data by analysis of variance were performed in order both to obtain a preliminary optimization of the operating conditions and to take into account the intrinsic sample heterogeneity associated to each specific procedure. Comparisons among three different preparations denoted that in the investigated conditions two-step preparations give larger yields of activated solid in comparison with single-step preparation. Preliminary optimized conditions denoted final solid yields (80–86%) for both two-step procedures. The effect of operating conditions on the chemical, structural and electrochemical properties of CMDs produced in preliminary optimised conditions was investigated and compared with those of a commercial EMD sample by acid and acid-reducing leaching for Mn speciation in solid phase, potentiometric titrations, X-ray and IR spectra and cyclic voltammetry. These characterisation tests denoted the significant effect of acid activation in both preparation procedures to obtain CMD samples with high % of Mn(IV)oxides. Potentiometric titrations of solid samples obtained by first and second steps denoted that both procedures gives two CMD samples with the same acid–base properties, which in comparison with commercial EMD present a residual dissociation in the basic pH range (similar structure and proton insertion properties for CMDs and EMD, but different structural defects). X-ray and IR spectra of solid samples by first and second steps denoted highly disordered systems and the presence of Mn_2O_3 in first step products and of γ-MnO_2 in second step product. Voltammetric cycles denoted that CMD samples obtained after acid digestion present similar peaks than commercial EMD but with higher current intensity.

Keywords: Chemical manganese dioxide; Factorial designs; Solid characterisation

1. Introduction

1.1. Applications and productions of manganese dioxides

Synthetic manganese dioxides found application in different production fields. From a commercial point of view the most important Mn dioxides are those that are electrochemically active and therefore used in dry cell batteries. Another commercial form is used in the manufacture of high-purity manganese oxides as ferrites and thermistors for the electronic industry. Manganese dioxides have been also increasingly used as oxidation catalysts, especially for air pollution abetment (removal of volatile organics, destruction of ozone).

Synthetic manganese dioxides can be prepared for different specific end uses either by chemical procedures (chemical manganese dioxide, CMD) or by electrochemical methods (electrolytic manganese dioxide, EMD) starting from Mn salts or solutions (leach liquors) or thermal activated products of natural ores.

Chemical manganese dioxide for dry cell batteries can be produced by heating $MnCO_3$ (with air at 320 °C), obtaining a higher manganese dioxide (approximate composition $MnO_{1.85}$) and completing oxidation by treatment with $NaClO_3$ in presence of sulphuric acid (Sedema process). Other methods for

* Corresponding author. Tel.: +39 06 49913333; fax: +39 06 490631.
E-mail address: francesca.pagnanelli@uniroma1.it (F. Pagnanelli).

0378-7753/$ – see front matter © 2007 Elsevier B.V. All rights reserved.
doi:10.1016/j.jpowsour.2007.01.066

the preparation of active manganese dioxide involve the oxidation of Mn(II) salts by using different oxidants such as $KMnO_4$, $NaClO_3$ and O_3 [1].

Electrolytic manganese dioxide can be produced by purified manganese sulphate solutions, acidified by H_2SO_4 and subjected to electrolysis at 90–98 °C. By this way MnO_2 is deposited (14–20 days) as a solid coating on the anode with yields ranging from 70 to >90%. Nowadays this technology is generally employed for synthetic manganese dioxide used in the manufacture of dry cells and electronic materials such as ferrites. Nevertheless the need for simple production equipments and low energy and time consuming processes re-directs the attention also towards the optimisation of other chemical productions [1–5] also taking into account the constant increase of oil cost and that the production of primary alkaline cell batteries requires up to 10 times energy consumption of the expected energy output [1]. In this contest the optimisation of the operating conditions in CMD production should be strictly related to the product characterisation because even slight changes in the synthesis conditions can lead to manganese dioxide samples with different electrochemical properties [1,3]. This aspect is strictly related to the complexity of discharge mechanisms in dry cell batteries and also to the rich variety of allotropic polymorphs of MnO_2.

1.2. Electrochemical behaviour and mineral structure

The mechanism of MnO_2 discharge in alkaline electrolytes involves the insertion of an electron from the external circuit to reduce Mn^{4+} to Mn^{3+}. For charge electroneutrality, protons formed by water decomposition at the solid/electrolyte interface are also inserted in the structure. Electrons and protons diffuse under the gradient between the surface and the bulk through the tunnels of the crystallographic matrix by hopping between adjacent sites (oxygen ions for protons and Mn^{4+} ions for electron). This first electron homogeneous reduction continues until all Mn^{4+} is consumed, and then Mn^{3+} species (MnOOH) were reduced heterogeneously dissolution of solid MnOOH to $[Mn(OH)_6]^{3-}$, heterogeneous reduction to less soluble $[Mn(OH)_6]^{4-}$, and final precipitation of $Mn(OH)_2$ [6,7]:

$$\gamma\text{-}MnO_2 + H_2O + e^- \rightarrow MnOOH + OH^- \quad (1)$$

$$MnOOH + H_2O + e^- \rightarrow Mn(OH)_2 + OH^- \quad (2)$$

According to this mechanism, the electrochemical activity of manganese dioxide is especially connected to the crystal structure, the chemical purity and in particular to the cationic mobility in the structure itself (being the proton diffusion the rate limiting step of the previously described process) [6,7]. Allotropic polymorphs of MnO_2 differ in the distribution of Mn ions in the interstices of a more or less closed-packed network of oxygen atoms. More than 20 predominantly Mn(IV) oxide phases have been recognise as mineral species [8]. Among these γ-MnO_2 is commonly used as cathodic material for primary cell batteries. This specific allotropic phase can be described as hexagonal closed packed array of oxide anions, in which half of the octahedral sites are selectively filled with Mn(IV) ions.

Different models have been proposed in the literature to describe the structure of γ-MnO_2 in relation to the solid electroactivity. After studying X-ray diffraction patterns, De Wolff [9] described γ-MnO_2 structure as a random intergrowth of pyrolusite layers in a ramsdellite matrix. The introduction of pyrolusite domains into ramsdellite matrix generates two kinds of tunnels in the γ-MnO_2 structure: [1 × 1] tunnels in pyrolusite domains and [1 × 2] tunnels in ramsdellite domains. Structural studies and related models indicated that, within the range of useful potential for MnO_2 reduction, protons diffuse mainly along [1 × 2] tunnels in the ramsdellite domain.

Electroactivity related to ramsdellite was also modelled by Ruetschi [10] introducing a cation vacancy model which assumes non stoichiometry only in the cationic lattice of ramsdellite domains (such as Mn^{4+} vacancies and Mn^{4+} cations replaced by Mn^{3+} cations). For charge balance, Mn^{4+} vacancies result in structural water and in the presence of an initial proton concentration making ramsdellite electrochemically more active than pyrolusite [11].

The electrochemical behaviour of γ-MnO_2 was also successfully correlated to the mineral structure by introducing two structural defects in an idealised ramsdellite host phase. The first is based on the De Wolff disorder model and is related to the percent pyrolusite amount (P_r). The second defect is microtwinning (Tw), packaging faults which does not modify the oxygen sublattice and corresponds to simple change in the distribution of Mn^{4+}/vacancies within the octahedral voids of the anionic network [12]. These authors denoted possible relations between microtwinning and Mn^{4+} vacancies: microtwinning generates new local environments for manganese atoms located in the twinning plane. This arrangement with more short $Mn^{4+} - Mn^{4+}$ distances is expected to be less stable than regular geometry being a likely site for cationic defects.

The relative amounts of pyrolusite intergrowth can be determined from X-ray diffractograms measuring the position of the orthorhombic peak (1 1 0 line) in comparison with the calculated values (a shift to higher angle corresponds to higher Pr) [12,13].

Microtwinning defects can be denoted by the difference between the positions of 1 2 1/1 4 0 and 2 2 1/2 4 0 lines of ramsdellite: a narrowing of the distance between these couples of lines means an increase of Tw [12,14,15].

γ-MnO_2 samples can be then classified according to P_r and Tw showing that the most promising cathode materials are those with minimum P_r and maximum Tw [15] in comparison with commercial EMD, which are characterised by $P_r \cong 50$ and Tw > 50 [12].

1.3. Aim of the work

The aim of this study is investigating the effect of operating conditions on the electrochemical properties of chemical manganese dioxides for possible applications in dry cell batteries. Despite similar works reported in the literature [1–4], the effect of preparation conditions was studied by performing replicated full factorial designs, choosing the better operating

conditions by statistical analysis accounting for sample variability observed even in controlled conditions. On the base of preliminary data reported in the literature, three preparation procedures were tested: precipitation–oxidation by air plus acid activation, precipitation–oxidation by H_2O_2 plus acid activation, precipitation–oxidation by $KClO_3$. Solid samples (before and after acid activation) were characterised by X-ray and IR to identify the operative conditions in which electroactive γ-MnO_2 is produced in larger amounts. Potentiometric titrations and voltammetric tests were performed to denote possible correlations among surface groups, structural phase and electroactivity of the produced samples.

2. Materials and methods

2.1. Preparation procedures

Chemical manganese dioxide was prepared according to three procedures:

- Two-step-air preparation.
- Two-step-H_2O_2 preparation.
- One-step-$NaClO_3$ preparation.

Two-step procedures consisted of a first step precipitation in oxidising conditions giving a mixed oxide precipitate, which is subjected to a second step activation in hot acid medium. One-step procedure consisted only of a single precipitation step in hot acidic conditions.

Experimental procedures adopted for these preparations were detailed in Sections 2.1.1, 2.1.2 and 2.1.3. Specific operating conditions of preliminary tests and factorial designs were reported in Tables 1 and 2, respectively. The estimates of the main effect and interactions investigated in factorial designs, along with their significance were evaluated by analysis of variance (ANOVA) (Table 3) [16].

2.1.1. Two-step-air preparation

Ome hundred and fifty millilitres samples of a $MnNO_3$ solution (1.67 M) were used for two-step-air preparation. Each solution was kept at the selected level of pH conditions by manual additions of NaOH (1 and 5 M). Precipitation (I step) was performed under air flux (except as differently specified for set 1 in Table 1) at 25 °C under magnetic stirring for two hours. The solid was separated by centrifugation (10 min at 10,000 rpm) and dried in an oven at 70 °C for 48 h. Initial (C_0) and final (C^I) concentrations of Mn in the liquid phase were measured by an inductively coupled plasma spectrophotometer (ICP) to evaluate the solid yield of this first step:

$$R_1 = \frac{C_0V_0 - C^IV^I}{C_0V_0} \times 100 \quad (3)$$

where V_0 and V^I are the initial and final volumes of the solution.

The solid was activated (II step) by using 1 M HNO_3 (2 g of solid in 100 ml) at 90 °C under stirring for 1 h. After the

Table 1
Preliminary tests: operating conditions used in the two-step preparations (air-based and H_2O_2-based) and one-step chlorate preparation; relative yields of single steps (R_1 and R_2) and overall yields (R_{tot})

Preparation procedure	Literature conditions	Operating conditions for preliminary tests							
		Test	$[Mn(NO_3)_2]$ (M)	Air	pH	R_1 (%)	R_2 (%)		R_{tot} (%)
Two-step air preparaion (set 1)	$[Mn(NO_3)_2] = 1$ M, pH 7, $T = 25$ °C [2]	O_2 (a)	1.67	No	8	3			
		O_2 (b)	1.67	Yes	8	75	69		53
Preparation procedure	Literature conditions	Operating conditions for preliminary tests							
		Test	$[MnCl_2]$ (M)	1 M NaOH volume (ml)		1M H_2O_2 volume (ml)	R_1 (%)	R_2 (%)	R_{tot} (%)
Two-step H_2O_2 preparation (set 2)	$[MnCl_2] = 0.43$ M, $[H_2O_2] = 0.8$ M, pH not specified (1 g NaOH in 75 ml), T = not specified (warmed) [4]	H_2O_2 (a)	1	5 (pH 12)		25	49	50	24
		H_2O_2 (b)	0.45	3 (pH 10)		25	85	60	51
Preparation procedure	Literature conditions	Operating conditions for preliminary tests							
		Test	$[MnCl_2]$ (M)	$[NaClO_3]$ (M)		17 M HNO_3 volume (ml)			R_{tot} (%)
One-step chlorate preparation (set 3)	$MnCl_2{\cdot}4H_2O = 57$ g, $NaClO_3 = 69.5$ g, $T = 100$ °C, pH not specified (sufficient amount of concentrated acid nitric), N.B.: volume not specified [3]	$NaClO_3$ (a)	0.78	1.75		5			41
		$NaClO_3$ (b)	0.55	1.24		Drops			18

Table 2
Factorial designs: operating conditions used in the two-step preparations (air-based and H_2O_2-based) and one-step chlorate preparation: relative yields of single steps (R_1 and R_2) and overall yields (R_{tot})

Preparation	Factorial design		Test	Yields		
	A: pH	B: aeration		R_1 (%)	R_2 (%)	R_{tot} (%)
Two-step air preparation (set 4)	7	No	1_{air}	1		
			$1'_{air}$	1		
	8	No	a_{air}	7		
			a'_{air}	8		
	7	Yes	b_{air}	5		
			b'_{air}	6		
	8	Yes	ab_{air}	83	98	81
			ab'_{air}	82	96	79

Preparation	Factorial design		Test	Yields		
	A: volume (ml) of 1 M NaOH (pH)	B: volume (ml) of 1 M H_2O_2		R_1 (%)	R_2 (%)	R_{tot} (%)
Two-step H_2O_2 preparation (set 5)	2.5 (7.0) (6.9)	25	$1_{H_2O_2}$	82	64	53
			$1'_{H_2O_2}$	78	64	50
	5.0 (13.2) (12.9)	25	$a_{H_2O_2}$	100	71	71
			$a'_{H_2O_2}$	100	69	69
	2.5 (6.7) (7.2)	75	$b_{H_2O_2}$	83	83	69
			$b'_{H_2O_2}$	85	84	71
	5.0 (13.4) (13.2)	75	$ab_{H_2O_2}$	100	78	78
			$ab'_{H_2O_2}$	100	77	77

Preparation	Factorial design		Test	Yield
	B: $[ClO_3]$ (M)	C: temperature (°C)		R_{tot} (%)
One-step chlorate preparation (set 6)	0.6	50	1_{ClO_3}	5
			$1'_{ClO_3}$	4
	1.5	50	b_{ClO_3}	15
			b'_{ClO_3}	14
	0.6	90	c_{ClO_3}	6
			c'_{ClO_3}	6
	1.5	90	bc_{ClO_3}	12
			bc'_{ClO_3}	14

activation the solid was separated by centrifugation (10 min at 10,000 rpm), washed by distilled water to eliminate the acid excess and dried in a oven at 70 °C for 48 h. The final Mn concentration (C) in the acid medium was measured by ICP to evaluate the solid yield of this second step:

$$R_2 = \frac{C_0V_0 - C^{I}V^{I} - CV}{C_0V_0 - C^{I}V^{I}} \times 100 \quad (4)$$

where V^{I} and V are the initial and final volume of the solution used for activation.

Table 3
Analysis of variance and estimates of main effects and interactions for the experimental data of factorial designs (set 4, set 5 and set 6) using R_1, R_2 and R_{tot} as dependent variables

Preparation	Effects	ANOVA for R_1		ANOVA for R_2		ANOVA for R_{tot}	
		Estimates	F-test significance (%)	Estimates	F-test significance (%)	Estimates	F-test significance (%)
Two-step air preparation	A	39	100				
	B	42	100				
	AB	36	100				
Two-step H_2O_2 preparation	A	18	100	0	19	13	100
	B	2	84	13	100	13	100
	AB	2	84	6	100	6	100
One-step chlorate preparation	B					8	100
	C					0	46
	BC					1	90

2.1.2. Two-step-H_2O_2 preparation

Fifty millilitres samples of a $MnCl_2$ solution (0.43 M) were heated to 50 °C and added for H_2O_2 (variable volumes of a 1 M solution according to the investigated conditions reported in Tables 1 and 2) and for a standard solution of NaOH (drop wise additions of a 1 M solution, volumes according to investigated conditions in Tables 1 and 2). Precipitation (I step) was performed under magnetic stirring at 50 °C for 2 h. The solid was separated by centrifugation (10 min at 10,000 rpm), washed by distilled water and dried in a oven at 70 °C for 48 h. Initial (C_0) and final (C^I) concentrations of Mn in the liquid phase were measured by ICP to evaluate the solid yield of this first step (R_1 as in Eq. (3)).

The solid was activated (II step) according to the same procedure reported before for two-step-air preparation. The final Mn concentration (C) in the acid medium was measured by ICP to evaluate the solid yield of this second step (R_2 as in Eq. (4)).

2.1.3. One-step-$NaClO_3$ preparation

Three hundred millilitres samples of a $MnCl_2$ solution (0.96 M) were added with $NaClO_3$ (variable weight according to investigated conditions, Tables 1 and 2) and with HNO_3 (0.5 ml of a 65% concentrated solution, except as differently specified for set 3 in Table 1). Precipitation was performed in jacketed glass vessels under magnetic stirring for one hour at constant temperature by using a thermostatic bath (temperature values in Tables 1 and 2). After the reaction the solution was left to stay for 24 h. The solid was then separated by centrifugation (10 min at 10,000 rpm), washed by distilled water and dried in a oven at 70 °C for 48 h. Initial (C_0) and final (C) concentrations of Mn in the liquid phase were measured by ICP to evaluate the solid yield (R_{tot}). A unique equation can be used to evaluate both one-step yield and global two-step yield:

$$R_{tot} = \frac{C_0V_0 - C^IV^I - CV}{C_0V_0} \times 100 \quad (5)$$

where C^I and V^I are zero in the case of one-step preparation.

2.2. Preparation

CMD samples of both two-step productions were prepared according to the previously described procedures (Sections 2.1.2 and 2.1.3) using ab_{air} condition for two-step air preparation and $b_{H_2O_2}$ for two-step H_2O_2 preparation (see Table 2). Different batch productions of each preparation were performed using 250 ml of Mn(II) solutions. For each preparation procedure all the solids produced by the first step were washed by distilled water, joined together and dried in a oven at 70 °C for 48 h. Two pools of solid material (one for each preparation) were then obtained as representative of the first step product (CMO_{air} and $CMO_{H_2O_2}$). Particle size distribution of these pool was determined by an automatic sieve. Size-fractionated samples were used for the second step activation and/or for the characterisation tests as described in the following section.

2.3. Characterisation tests

2.3.1. Acid leaching and acid-reducing leaching

Acid leaching for the determination of Mn(II) in solid samples was performed by using the solids obtained from the first and second steps of both procedures. One-gram samples were suspended in 50 ml of deionised water with 5 ml of 17N H_2SO_4. The suspension was thermostated at 90 °C and kept under magnetic stirring for 12 h. The final product was diluted to a known volume, the residual solid (composed of Mn(IV) oxides not leached without a reducing agent) was separated by centrifugation, and Mn concentration in solution was determined by ICP.

Acid-reducing leaching for the determination of total Mn in CMO and CMD samples was performed as reported above for acid leaching with the only difference that also 1 g glucose was added as reducing agent according to the following global reaction stoichiometry [17]:

$$C_6H_{12}O_6 + 12MnO_2 + 24H^+ = 6CO_2 + 12Mn^{2+} + 18H_2O \quad (6)$$

Final Mn concentrations (determined as in the case of acid leaching) correspond in this case to Mn(II) plus Mn(VI).

Both acid and acid-reducing leaching were performed twice for each sample; medium values and maximum dispersions were reported in Table 4.

2.3.2. Potentiometric titrations

Solid samples obtained from the first and second steps of both procedures and a commercial EMD sample were potentiometrically titrated to determine their acid base properties. Two distinct suspensions were prepared for each solid samples (0.5 g of solid with particle size between 45 and 63 μm in 30 ml of deionised water). After preliminary fluxing by N_2 to remove CO_2, both suspensions obtained for each solid sample were titrated, one using 0.1N NaOH standard solution (positive abscissa axis in Fig. 2) and the other with 0.1N HCl standard solution (negative abscissa axis in Fig. 2). After each addition of titrant (NaOH or HNO_3) the pH of suspension was allowed to reach the equilibrium under magnetic stirring and then measured by a pH meter.

2.3.3. X-ray diffraction analyses

Solid samples obtained from the first and second steps of both procedures (size fractionated samples 45–63 μm) and a commercial EMD sample (with the same particle range) were analysed by X-ray diffraction.

Table 4
Total manganese and Mn(IV) contents in solid samples obtained by first step (CMO_{air}) and second step (CMD_{air}) of air-based preparation and by first step ($CMO_{H_2O_2}$) and second step ($CMD_{H_2O_2}$) of H_2O_2-based preparation

Preparation procedure	Samples	Mn_{tot} (%)	Mn(IV) (%)
Two-step-air preparation	CMO_{air}	40 ± 2	13 ± 6
	CMD_{air}	52 ± 3	97 ± 3
Two-step-H_2O_2 preparation	$CMO_{H_2O_2}$	37 ± 4	15 ± 5
	$CMD_{H_2O_2}$	54 ± 3	87 ± 3

2.3.4. IR spectroscopic analyses

IR spectra were performed by using KBr as transparent component for the dilution of solid samples produced by first and second steps of both procedures. Manganese oxide-bearing disk of KBr were prepared by two successive dilutions: 0.002 g samples of each solid (size fractionated samples 45–63 μm) were mixed with 0.3 g of KBr; 0.03 g of this mixture were diluted again with other 0.3 g of KBr. 0.15 g samples of this second mixture were pressed and used for disk preparation. The signals of CO_2 and aqueous vapour in the air and possible impurities of KBr were subtracted from all the spectra by collecting a background spectrum. Eight scansions between 400 and 4000 cm^{-1} were performed for each spectrum.

2.3.5. Cyclic voltammetry

Charge and discharge processes of commercial EMD and of solid samples from the first and second steps of both procedures were characterised by cyclic voltammetry by using a polarograph with two Zn electrodes (reference and auxiliary) in 0.1 M $ZnSO_4$ alkaline solution (0.1 M KOH). The working electrode was prepared by mixing the solid sample to be tested (45–63 μm) with graphite and polyvinyl fluoride with the following proportion in weight 8:2:2 (weight of EMD and CMD samples used for electrode preparation 0.080 ± 0.05 g). The mixture obtained was pressed over a platinum disk electrode [18]. Potential scansions during voltammetric cycles were performed in the range 1.7–0.8 V at a speed of 2 mV s^{-1}.

3. Results and discussion

3.1. Preliminary tests

Manganese speciation in different operating conditions of pH and potential denotes that different degrees of oxidative conditions are required for the productions of Mn(IV) oxides as pH changes (Fig. 1). In particular in 7–0 pH range the empirical correlation between Eh and pH for the low boundary limit of potential in solution (Eh_{LB}) can be calculated from speciation diagram (Fig. 1A) as $Eh_{LB} = -0.0592\,pH + 0.9726$. For each pH in solution Eh should be larger than the calculated Eh_{LB} to avoid the precipitation of oxides with Mn oxidation number lower than 4 (i.e. Mn_3O_4 and Mn_2O_3). Simultaneous precipitation of these Mn oxides determines the necessity of the secondary acid activation in order to oxide and dissolve lower Mn compounds:

$$MnO_{2-n} \times MnO_2 + 2HNO_3 = Mn(NO_3)_2 + n(\gamma\text{-}MnO_2) + H_2O \quad \text{with } 0.2 < n < 0.4 \tag{7}$$

Speciation diagrams also denotes that working in the acidic pH range higher potential conditions in solution are required but the precipitation of Mn oxides different from MnO_2 is avoided working below pH 5 (Fig. 1B). Consequently, the precipitation of Mn oxides in acidic conditions do not require successive activation procedure.

The analysis of these speciation diagrams suggests two main operative possibilities for increasing MnO_2 yields during precipitation from Mn(II) solutions:

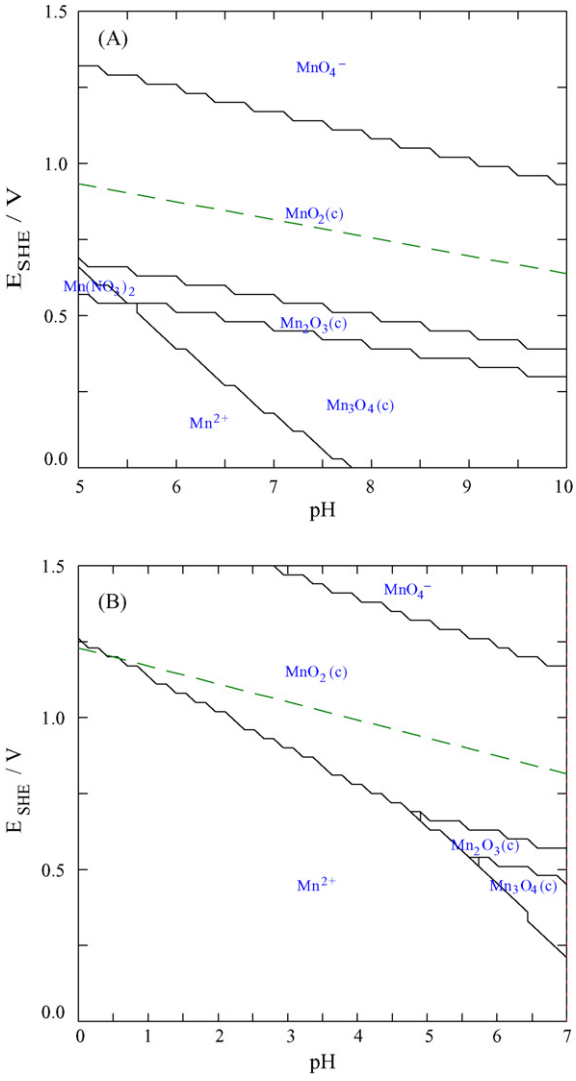

Fig. 1. Predominance diagrams Eh vs. pH for manganese species in two different solution systems: 1 M $Mn(NO_3)_2$ (A) and 0.3 M $MnCl_2$ + 0.7 M $NaClO_3$ (B).

- Using high potential conditions in alkaline pH range to reduce the precipitation of less oxidised Mn oxides.
- Working in acidic conditions with strong oxidants to avoid the following acid activation.

MnO_2 precipitation in alkaline conditions reported in the literature [2] does not account for possible variation of potential conditions in order to increase Mn oxidation state in the solid. In this paper the precipitation of Mn is performed in improved oxidative conditions by forced aeration and addition of H_2O_2.

3.1.1. Two-step-air preparation

A preliminary validation of the advantages of aeration during precipitation was found by performing Mn precipitation in conditions similar to those reported in the literature [2] with and without aeration (set 1 tests in Table 1). In this case the aeration determines a significant increase of the yield of the first step, R_1 (Eq. (3)). In particular without aeration R_1 is 3% and with aeration becomes 75%.

The confirmation of the effective increase of Mn oxidation state in the solid obtained with aeration is given by the yield after second step of activation (R_2). In fact the precipitated obtained with aeration was only partially dissolved during acid activation ($R_2 = 69\%$) denoting a high percentage of MnO_2, which necessitates a reducing agent to be dissolved.

According to these preliminary results, the following factorial design aims to optimise this two-step production with particular attention to the effect of pH and aeration (set 4 in Table 2). The temperature during the first step was kept constant at 25 °C according to the literature results showing that the oxidation degree of precipitated Mn oxides conditions is inversely proportional to the rate of precipitation which decreases lowering the temperature [2] (Table 1).

3.1.2. Two-step-H_2O_2 preparation

Preliminary tests were performed to evaluate possible applications of H_2O_2 (set 2 tests in Table 1). These tests denoted the positive effect of increasing H_2O_2/Mn ratio with R_1 changing from 49 to 85% and with similar values for the second step (50–60%).

According to these preliminary results, the following experimental design aims to optimise this two-step production with particular attention to the effect of pH and oxidant concentration (set 5 in Table 2), while the temperature during the first step precipitation was chosen at 50 °C according to the literature [4] (Table 1).

3.1.3. One-step-$NaClO_3$ preparation

CMD in acidic conditions by a single step precipitation was attempted by using sodium chlorate as oxidant agent in solution according to literature data [3], which denoted that sodium salt gave better results for γ-MnO_2 production with respect to $KClO_3$. Using the experimental conditions analogous to those reported in the literature (set 3 tests in Table 1) a strong effect of pH was observed on the solid yield (R_{tot}). Single step production yield is 40% for pH 2 and 17% for pH 0, lower than the overall yields of the two-step procedures (77 and 66–76% by using aeration and H_2O_2, respectively).

According to these preliminary results, the following factorial design aims to optimise the single-step production with particular attention to the effect of the temperature and oxidant concentration (set 6 in Table 2) on the chemical and electrochemical characteristics of the Mn oxides produced. In this case the effect of temperature was also considered aiming to reduce both energy consumption and the rate of gas dispersion generated by chlorate reduction. pH was kept at 0 according to preliminary data showing a strong reduction of solid yield for pH raising from 0 to 2.

3.2. Factorial designs

3.2.1. Two-step-air preparation

Experimental data from replicated factorial design for Mn oxides precipitation (set 4 in Table 2) clearly show the synergic effect of pH and aeration on the solid yield (R_1) for the first step of air-based procedure.

Statistical significance for each main factor and interaction confirm this obvious results showing the 100% significance for F-tests related to mean square estimates of ANOVA (Table 3). This finding is in agreement with Mn speciation reported in Fig. 1A showing that Mn oxide precipitation prevails for simultaneous basic pH and oxidative conditions. Even though all main factors and interaction are significant (their change from lower to higher level causes a significant yield increase), only *ab* conditions allow semi-quantitative Mn precipitation.

Second step activation was performed only for ab_{air} and ab'_{air} samples neglecting the other samples because of the very low yield not suggesting practical applications for those conditions. The high yields associated with acid activation mean that the quite totality of Mn oxides precipitated in the first step were already mainly made up of Mn(IV) oxides, not dissolved during acid treatment (see also characterisation by acid leaching and acid-reducing leaching, Section 3.4.1).

At this stage ab_{air} combination was then chosen in the following preparation of CMD samples for two-step-air procedure.

3.2.2. Two-step-H_2O_2 preparation

Experimental data from replicated factorial design for Mn oxides precipitation with H_2O_2 (set 5 in Table 2) show that quantitative solid yields can be obtained for $a_{H_2O_2}$ and $ab_{H_2O_2}$ conditions. ANOVA confirms that factor A (pH) is the only factor whose change in the investigated range causes a significant increase of the yield R_1. Nevertheless not only solid yield but also solid characteristics should be evaluated for the optimisation of operating conditions. In particular the colour of the solid samples obtained by this procedure in the different conditions can be a clearly hint of the chemical composition of the solids. In fact pure Mn(IV) oxides are dark black coloured, while light brown-reddish samples are generally characterised by hydrated oxides with oxidation number lower than 4. The colour of the samples obtained from first step of set 5 tests were light brown for $1_{H_2O_2}$ and $a_{H_2O_2}$ conditions, dark brown for $b_{H_2O_2}$ and reddish for $ab_{H_2O_2}$. This means that the conditions giving the largest yield of solid ($a_{H_2O_2}$ and $ab_{H_2O_2}$) are not the same characterised by the darkest solid ($b_{H_2O_2}$). The choice of the best conditions for this procedure was then also based on the results of the second step activation. The largest yields R_2 associated to $b_{H_2O_2}$ condition confirmed the chromatic hint from first step solids. ANOVA confirms this result showing that only B main effect factor and AB interaction are significative (F-test significance larger than 95%). According to these finding $b_{H_2O_2}$ condition was chosen for CMD preparation by two-step-H_2O_2 procedure.

3.2.3. One-step-$NaClO_3$ preparation

Experimental data from replicated factorial design for CMD preparation with $NaClO_3$ (set 6 in Table 2) show that very low solid yields were obtained in all the investigated conditions. Even though the solids produced in b_{ClO_3}, c_{ClO_3} and bc_{ClO_3} conditions are dark black and ANOVA results suggest possible yield improvement by increasing ClO_3 concentration (B is the only significant factor for set 6 tests), the advantages of using a single step procedure instead of two-step ones seem not to be sufficient to continue experiments with chlorate, also con-

sidering the environmental concerns related to this reagent. For this reasons single-step-chlorate procedure was not used in the following preparation and characterisation phases of CMD.

3.3. Preparation of CMD samples

CMD samples were prepared according to ab_{air} condition for two-step air preparation and $b_{H_2O_2}$ for two-step H_2O_2 preparation (Table 2). It is noteworthy remembering that the solids obtained by different batches of each procedure were joined together to obtain a pool of material representative not only of the specific procedure, but also of the intrinsic variability associated to each preparation procedure. Solid samples obtained from the first steps (generic chemical manganese oxides, CMO_{air} and $CMO_{H_2O_2}$) and the second steps (chemical manganese dioxides CMD_{air} and $CMD_{H_2O_2}$) of both procedures were characterised in the follow according to different experimental tests in order to evaluate their characteristics and performances in comparison with commercial sample of EMD.

3.4. Characterisation of CMD samples

3.4.1. Mn speciation in the solid samples by acid and acid-reducing leaching

Solid samples obtained from the first and second steps of both procedures were leached in acid medium with and without glucose to determine total manganese amount (Mn_{tot}) and its speciation as Mn(IV) and Mn(II). The amount of Mn(IV) can be obtained as the difference between the total manganese extracted by acid-reducing leaching and Mn(II) dissolved by acid leaching (Mn(IV) cannot be dissolved without a reducing agent).

Percent compositions of manganese as total and Mn(IV) for the four CMD samples were reported in Table 4. Experimental data denoted the significant effect of acid activation in both procedures in order to augment final percent of Mn(IV) in solid samples.

3.4.2. Surface acidity by potentiometric titrations

Surface characterisation by potentiometric titration have been considered to investigate and to enhance the rate of charge-transfer process at the solid/electrolyte interface. In fact taking into account that proton diffusion is the rate-limiting step of the previously described discharge process, knowledge of acid surface properties and correlation with bulk crystal structure and electroactivity can guide the optimisation of the preparation procedures. Metal oxides as manganese dioxides in presence of water tend to form surface hydroxyl groups with acid and basic properties (dissociative chemisorption) [6,19] and different degree of polarization depending on different factors such as metal ion coordination and metal–oxygen bond length [20].

Experimental results of potentiometric titrations of the solid samples obtained by first step (CMO_{air}) and second step (CMD_{air}) of air-based preparation and by first step ($CMO_{H_2O_2}$) and second step ($CMD_{H_2O_2}$) of H_2O_2-based preparation were reported in Fig. 2A and B, respectively. The effect of activation on the acidic properties of the surface functional groups was analysed using EMD titration as a standard reference of

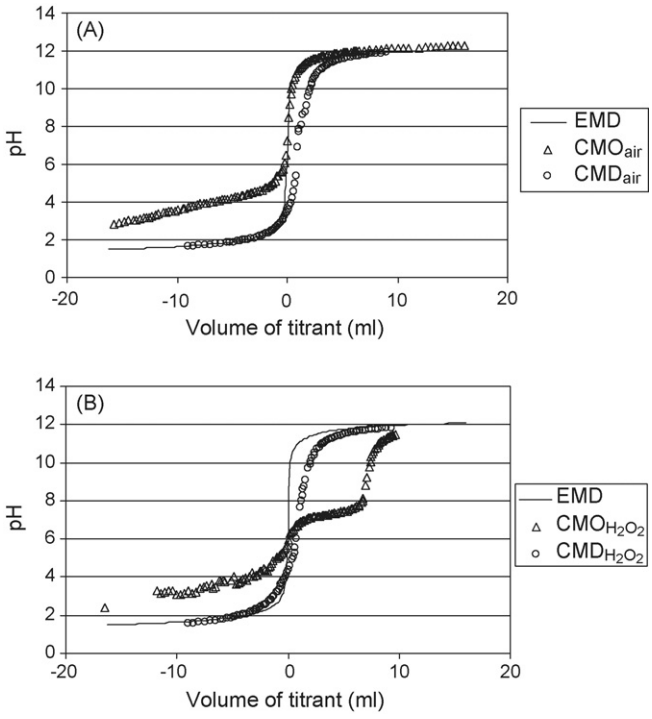

Fig. 2. Potentiometric titrations of EMD and solid samples obtained by first step (CMO_{air}) and second step (CMD_{air}) of air-based preparation (A) and by first step ($CMO_{H_2O_2}$) and second step ($CMD_{H_2O_2}$) of H_2O_2-based preparation (B). Negative part of abscissa axes refers to acid titrant additions and positive part to basic titrant addition.

final desired characteristics. In particular EMD titration does not denote distinct flex points resembling sites dissociation, meaning that in the investigated range of pH this test cannot reveal significant dissociation reactions (continuous line in Fig. 2). On the other side considering the samples of CMD produced, this characterisation test denoted the dissociation of weakly acidic sites both in acid and basic range. This is in agreement with other titration curves reported in the literature [19] also showing that surface hydroxyl groups of MnO_2 oxides (≡MnOH) can act as acids at high pH (Eq. (8)) and as bases at low pH (Eq. (9)):

$$\equiv \mathrm{MnOH} \leftrightarrow \equiv \mathrm{MnO^-} + \mathrm{H^+} \quad (8)$$

$$\equiv \mathrm{MnOH} + \mathrm{H_2O} \leftrightarrow \equiv \mathrm{MnOH_2^+} + \mathrm{OH^-} \quad (9)$$

In particular it is possible to observe that:

- Solid samples after the first step of both procedures present active sites dissociating in the acidic range (the pH values of the negative abscissas of CMO_{air} and $CMO_{H_2O_2}$ are larger than that of EMD meaning that the acid titrant added gives a final pH larger than that of EMD because of reaction with solids, i.e. partial dissolution of Mn(II)oxides and protonation of ≡MnOH groups to $\equiv MnOH_2^+$).
- In the basic pH range CMO_{air} presents an experimental trend which is very similar to that of EMD, while $CMO_{H_2O_2}$ strongly differs denoting a distinct flex point at pH around 7.
- Solid samples after the second step of both procedures present quite identical acid–base properties among them, perfectly

resembling EMD in acid range and with residual dissociation in the basic range (the pH values of the positive abscissas of CMD_{air} and $CMD_{H_2O_2}$ are lower than that of EMD meaning that the basic titrant added reacted with surface sites which dissociate in the basic range giving a pH lower than that of EMD).

Considering that hydroxyl groups dissociating in acid pH are the basic groups and that hydroxyl groups reacting in the acid pH are the basic groups, both CMD samples present basic groups properties similar to those of EMD while some differences emerge for the acidic sites. Malloy et al. [6] found that acidic strength of hydroxyl groups can be related to defects in the structure (as Mn^{3+}) and cation vacancies, while basic groups activity is dependent by structural properties of bulk phase. According to these correlations the produced CMD samples would present structural properties similar to EMD (same titration profiles in acid region) and would differ regarding the defects of such structure (different titration profiles in basic region). Nevertheless Malloy et al. [6] also found that in alkaline conditions proton insertion mainly occurs by the action of basic hydroxyl groups which present similar properties for EMD and CMD samples. These preliminary observation about structural and electrochemical properties are further addressed by other tests of characterisation reported in the following section.

3.4.3. X-ray diffractograms

X-ray analyses denoted highly disordered structures for the solids obtained from the first and second steps of both procedures. In particular CMO_{air} and $CMO_{H_2O_2}$ diffractograms (data not reported here) do not present the typical signals of γ-MnO_2, but are characterised by some similarities with other Mn oxides classified in the literature as Mn_2O_3 [13]. Both activated samples (CMD_{air} and $CMD_{H_2O_2}$) present the characteristic peaks of γ-MnO_2 for (1 1 0), (0 2 1), (1 2 1/1 4 0) and (2 2 1/2 4 0) lines [7,14] (Fig. 3). In particular the wide shape of (1 1 0) line peak and its shifting towards high angles (up to 25° against a calculated value of 22° [7]) denoted high pyrolusite amounts.

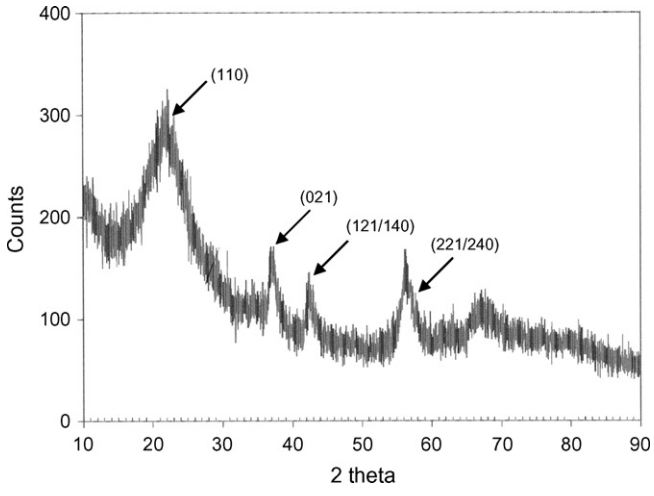

Fig. 3. X-ray spectra for solid samples obtained by second step ($CMD_{H_2O_2}$) of H_2O_2-based preparation.

In addition both lines (1 2 1/1 4 0) and (2 2 1/2 4 0) are single peaks confirming the high structural disorder associated with microtwinning defects [14,21].

3.4.4. IR spectra

Considering that X-ray powder diffraction analysis of γ-MnO_2 are characterised by poor quality and a number of sharp and broad peaks over a diffuse background noise, IR spectroscopy analysis can be an alternative or a supplement to X-ray being sensitive also to amorphous components and to the structural environment of the hydrous components, which can be diagnostic for a specific mineral phase of MnO_2 [8]. IR of manganese dioxides can denote the presence of OH groups and H_2O as bound water in the mineral structure (adsorption around 3400 and 1620 cm^{-1}), while the bands in the region 1000–400 cm^{-1} reveal information about MnO_6 octahedra. In particular OH bending vibration at 1620 cm^{-1} was considered characteristic of the structural water in ramsdellite domains of γ-MnO_2 and distortions in MnO_6 octaedra (and the associated partial amorphisation typical of highly performing samples) could be recognised in the 1000–400 cm^{-1} region in comparison with natural nsutite samples [8,22].

IR spectra of the solids obtained from the first and second steps of both procedures present intense peaks at 3430 and 1634 cm^{-1} related to OH stretching and bending, respectively (Fig. 4).

IR spectra of CMO_{air} and $CMO_{H_2O_2}$ samples were both characterised by distinct peaks at 525 and 630 cm^{-1} due to different valence of Mn in the solid structure [22] in accordance with Mn_2O_3 identification by X-ray. In the range 500–800 cm^{-1} CMD_{air} and $CMD_{H_2O_2}$ are characterised by large bands considered as characteristics of γ-MnO_2 [2].

The intense peak at 1384 cm^{-1} can be associated to the interaction of Mn with surrounding species such as O, OH, H^+ and K^+, with larger peak intensities in CMD than in CMO related to higher electrochemical activities [22].

3.4.5. Voltammetric cycles

Voltammetry is the most powerful tool for assessing the electrochemical activity of manganese oxides. In particular the shape, the number and the position of the different peak resembling the redox processes can provide additional information for material characterisation and selection of production methods.

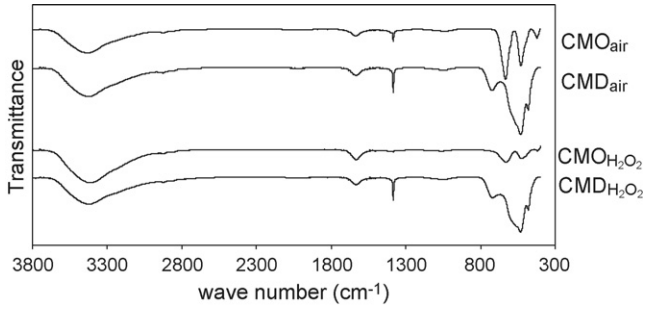

Fig. 4. IR spectra for solid samples obtained by first step (CMO_{air}) and second step (CMD_{air}) of air-based preparation and by first step ($CMO_{H_2O_2}$) and second step ($CMD_{H_2O_2}$) of H_2O_2-based preparation.

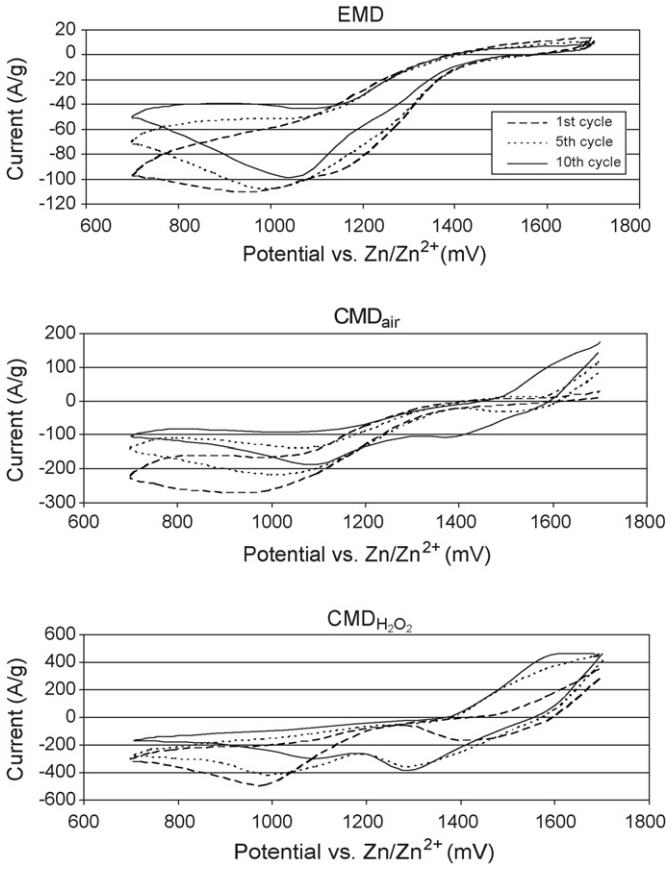

Fig. 5. Voltammetric cycles for solid samples obtained by first step (CMO_{air}) and second step (CMD_{air}) of air-based preparation and by first step ($CMO_{H_2O_2}$) and second step ($CMD_{H_2O_2}$) of H_2O_2-based preparation (current is normalised to mass of manganese oxides used for electrode preparation).

According to two-step discharge mechanism (Eqs. (1) and (2)), γ-MnO_2 reduction is generally characterised by two or three cathodic peaks: in alkaline solutions the first step is observed in the range between 200 and −350 mV (multiple signals), and the second step between −350 and −850 mV by using Hg/HgO/9N KOH as reference electrode [13,18,23–27].

Cyclic voltammetry was then chosen for the preliminary electrochemical characterisation of CMD samples in comparison with commercial EMD. In Fig. 5A the first, the fifth and the 10th cycle obtained for EMD were reported. The shape of the cycle is strongly dependent on the number of cycle. The current intensity of each cycle peak diminishes during the test probably because of significant loss of material due to Mn(III) dissolution, but also for the formation of heteroalite ($ZnMn_2O_4$) not as easily discharged as MnOOH and thus increasing cell impedance [28]. The discharge process is characterised by a wide peak ranging from 900 to 1200 mV being the composition of two distinct peaks with the high-voltage component becoming less intense with respect to the low-voltage, as cycling goes on. This behaviour has been already observed for manganese dioxide samples [18,27] and can be explained by assuming that the two peaks around 1200 and 1000 mV are related to the two reduction steps of MnO_2 (Eqs. (1) and (2)). These peaks have been observed in a wide range of potential values also depending on the analytical technique used for voltammetric characterisation. Using similar experimental equipments (abrasive stripping voltammetry) with Hg/HgO/9N KOH reference electrode I step is generally observed between 0 and −200 mV and the II step between −200 and −400 mV [18,27]. Considering an approximate equivalence of −400 mV versus Hg/HgO/9N KOH reference electrode to 1000 mV of an alkaline Zn–MnO_2 cell [13] the peak observed at 1000 mV in our system (resembling cell components) corresponds to −400 mV peak obtained with Hg/HgO electrode and then to the II step, and analogously the peak at 1200 corresponds to that at −200 versus Hg/HgO and then to the I step. This association even if coming from approximate assumptions seems to be quite reasonable and also in accordance with the inversion of intensity of the two peaks observed during cycling. This finding was already observed during abrasive stripping voltammetry of MnO_2 samples and can be explained by taking into account the specific electrode preparation technique [18,27]. In fact using compressed assembly of CMD particles enhances the diffusion of dissolved $[Mn(OH)_6]^{3-}$ favouring the II step reduction in comparison with composites electrodes.

Fig. 5B and C reports voltammetric cycles for activated CMD samples obtained from preliminarily optimised preparation conditions using air and H_2O_2 as oxidants (CMD_{air} and $CMD_{H_2O_2}$). Voltammetric cycles on the same samples before acid treatment (experimental data not reported here) do not show any distinct peak confirming the importance of the second activation step for CMD electrochemical properties. CMD samples present a strong variability during cycling with the I reduction process ranging from 1550 to 1300 mV and the II reduction process from 1080 to 920 mV. Some oxidation signals are also observable for CMDs around 1500–1600 mV. As in the case of EMD the current intensity reduced as cycling proceeds, but both CMD samples are characterised by larger current intensity. Even thought peak intensity can be related to solid powder amount used for electrode preparation [18], the observed differences cannot be explained only by this effect considering the accuracy in electrode preparation. Larger current intensity associated to CMD samples with respect to commercial EMD can be considered a favourable characteristic of the prepared samples themselves, perhaps correlated with the structural defects characteristic of CMD samples as denoted by potentiometric titration.

Capacity values ($Ah\,g^{-1}$) have been evaluated by the area of the voltammetric cycles for the three different materials. The specific values calculated from the first cycle for each material were 5.9 $Ah\,g^{-1}$ for EMD, 9.2 $Ah\,g^{-1}$ for CMD_{air} and 15.9 $Ah\,g^{-1}$ for $CMD_{H_2O_2}$, showing the good performances of the prepared materials in comparison with the commercial one. Dynamic trends of capacity were also calculated for the following cycles and reported in Fig. 6. It is possible to note that CMD_{air} presented a quite constant trend with values slightly exceeding the commercial EMD sample. On the other hand, $CMD_{H_2O_2}$ capacities were characterised by a steep increase and since the fifth cycle by a plateau at $29.9 \pm 0.4\,Ah\,g^{-1}$. This improvement of capacity for $CMD_{H_2O_2}$ sample could be due to the lower percentage of Mn(IV) with respect to CMD_{air} (Table 4) according to other findings reported in the literature, showing that partially reduced samples of MnO_2 improved both the reversibility and the capacity of the manganese electrode [24].

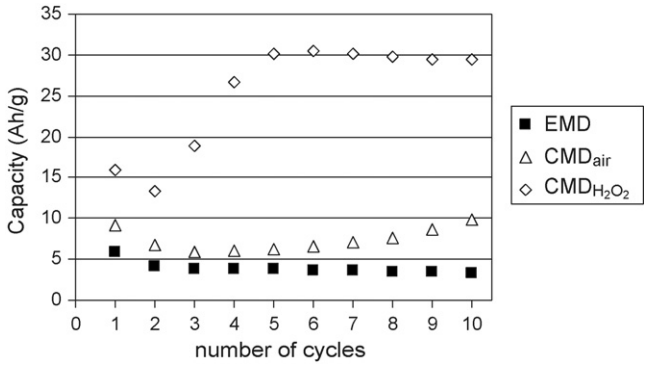

Fig. 6. Capacity of EMD and CMDs calculated for the different voltammetric cycles.

4. Conclusions

Experimental designs by replicated factorials and related statistical analysis by ANOVA allowed the optimization of the operating conditions for different CMD preparations also taking into account the intrinsic sample heterogeneity associated to each specific procedure. Comparisons among three different preparations denoted that in the investigated conditions two-step preparations give larger yields of activated solid in comparison with single-step preparation. Preliminary optimized conditions denoted similar final yields for both two-step procedures ranging from 80 to 86%.

Main findings by characterisation tests for solid samples obtained in the chosen conditions for both procedures can be resumed as follows:

- Mn speciation in solid phase by acid and acid-reducing leaching denoted the significant effect of acid activation in both preparation procedures to obtain CMD samples quite completely made up of Mn(IV)oxides.
- Potentiometric titrations of solid samples obtained by first and second steps denoted that both procedures gives two CMD samples with the same acid–base properties, which in comparison with commercial EMD present a residual dissociation in the basic pH range (similar structure and proton insertion properties for CMDs and EMD, but different structural defects).
- X-ray and IR spectra of solid samples by first and second steps denoted highly disordered systems and the presence of Mn_2O_3 in CMO_{air} and $CMO_{H_2O_2}$ and of highly disordered γ-MnO_2 in both CMD_{air} and $CMD_{H_2O_2}$.
- Voltammetric cycles denoted that CMD samples obtained after acid digestion present similar peaks than commercial EMD but with higher current intensity.

The preliminary results reported in this work denoted that Mn(IV) samples obtained by chemical oxidation in preliminary optimised conditions present similar properties of those of a commercial EMD sample in terms of acid–base properties, chemical and structural composition and electroactivity. This encourages further tests in order to improve product yields and characteristics and to compare EMD and CMD processes in terms of economics and environmental impacts by life cycle assessment.

Acknowledgments

Authors are grateful to Prof. Ruggero Caminiti and Mr. Claudio Cozza for their helpful collaboration in the experimental work.

References

[1] S.W. Donne, G.A. Lawrence, A.J. Swinkels, Mater. Res. Bull. 30 (1995) 859–869.
[2] Y.V. Kuz'minskii, A.A. Andriiko, L.I. Nyrkova, J. Power Sources 52 (1994) 49–53.
[3] J.B. Fernandes, B. Desai, V.N. Kamat Dalal, Electrochim. Acta 28 (1983) 309–315.
[4] K.K. Sen Gupta, B.A. Bilkins, Carbohyd. Res. 315 (1999) 70–75.
[5] L. Yuan, Z. Li, J. Sun, K. Zhang, Y. Zhous, Mater. Lett. 57 (2003) 1945–1948.
[6] A.P. Malloy, G.J. Browning, S.W. Donne, J. Colloid Interf. Sci. 285 (2005) 653–664.
[7] D. Qu, Electrochim. Acta 49 (2004) 657–665.
[8] R.M. Potter, G.R. Rossman, Am. Miner. 64 (1979) 1199–1218.
[9] P.M. De Wolff, Acta Cryst. 12 (1959) 341–345.
[10] P. Ruetschi, J. Electrochem. Soc. 131 (1984) 2737–2744.
[11] D. Balachandran, D. Morgan, G. Ceder, A. van de Walle, J. Solid State Chem. 173 (2003) 462–475.
[12] Y. Chabre, J. Pannetier, Prog. Solid State Chem. 23 (1995) 1–130.
[13] D.K. Walanda, G.A. Lawrence, S.W. Donne, J. Power Sources 139 (2005) 325–341.
[14] L.I. Hill, A. Verbaere, D. Guyomard, J. Power Sources 119-121 (2003) 226–231.
[15] K.S. Abou-El-Sherbini, J. Solid State Chem. 166 (2002) 375–381.
[16] D.C. Montgomery, Design and Analysis of Experiments, John Wiley & Sons, 1991.
[17] M. Trifoni, F. Vegliò, G. Taglieri, L. Toro, Miner. Eng. 13 (2000) 217–221.
[18] D.A. Fiedler, J.O. Besenhard, M.H. Fooken, J. Power Sources 69 (1997) 157–160.
[19] H. Tamura, T. Oda, M. Nagayama, R. Furuichi, J. Electrochem. Soc. 136 (1989) 2782–2786.
[20] J. Westall, H. Hohl, Adv. Colloid Interf. 12 (1980) 265–294.
[21] J.R. Hill, C.M. Freeman, M.H. Rossouw, J. Solid State Chem. 177 (2004) 165–175.
[22] M.V. Ananth, S. Pethkar, K. Dakshinaurthi, J. Power Sources 75 (1998) 278–282.
[23] G.G. Kumar, S. Sampath, Solid State Ionics 160 (2003) 289–300.
[24] X. Xia, C. Zhang, Z. Guo, Z. Liu, G. Walter, J. Power Sources 109 (2002) 11–16.
[25] V.K. Nartey, L. Binder, A. Huber, J. Power Sources 87 (2000) 205–211.
[26] W. Jantscher, L. Binder, D.A. Fiedler, R. Andreaus, K. Kordesh, J. Power Sources 79 (1999) 9–18.
[27] D.A. Fiedler, J. Solid State Electrochem. 2 (1998) 315–320.
[28] D. Linden, Handbook of Batteries and Fuel Cells, 1984.